Pergamon

Int. J. Heat Mass Transfer. Vol. 39, No. 14, pp. 2989–3002, 1996

0017-9310/96 $15.00 + 0.00

0017-9310(95)00344-4

A review of semi-analytical solutions for flame impingement heat transfer

CHARLES E. BAUKAL and BENJAMIN GEBHART

Department of Mechanical Engineering and Applied Mechanics, University of Pennsylvania, Philadelphia, PA 19104-6315, U.S.A.

(*Received* 6 *April* 1995 *and in final form* 12 *September* 1995)

Abstract—Twelve experimental flame impingement heating studies are reviewed. The targets were cylinders, flat plates and hemi-nosed cylinders. Forced convection (laminar and turbulent) and thermochemical heat release, have been the most important heat transfer processes. Several semi-analytic solutions have been developed, for the heat flux to the forward stagnation point of a body of revolution. These were originally developed for aerospace applications, such as rocket re-entry into the earth's atmosphere. These solutions, and many variations, have been used to simulate flame impingement heat transfer. The results of sample calculations are compared to some of the experimental measurements. Copyright © 1996 Elsevier Science Ltd.

1. INTRODUCTION

Heat transfer from high temperature gases, to axisymmetric and blunt-nosed bodies, has been studied for many years. These processes are very important in aerospace applications. Aerospace vehicles, such as rockets and missiles, travel at high supersonic velocities. Commonly, the nose of these surfaces is axisymmetric, blunt, and rounded. Gas shock-waves are produced as the vehicles travel through the atmosphere. The resulting temperatures at the stagnation point are generally high enough to cause the atmospheric gases to dissociate into many chemical species. Very high heat fluxes arise in that region. Several semi-analytic solutions have been proposed for calculating such fluxes. Those solutions were derived from the laminar, two-dimensional (2D), axisymmetric, boundary layer equations, applied in the stagnation region. The equations were simplified using similarity flow formulations. In the resulting heat flux solutions, a constant was numerically determined. Therefore, the solutions are referred to as semi-analytic.

The heat transfer from impinging, chemically active, flames has also been extensively studied. The experimental conditions and measurements, for those studies, have been previously reviewed [1, 2]. In twelve of those studies [3–14], the measured heat flux was compared against one or more semi-analytic solutions. The stagnation body has commonly been a hemispherically-nosed cylinder (see Fig. 1). This geometry has been used, because of its similarity to the shape of aerospace vehicles. Then, the semi-analytic heat transfer solutions, derived for aeronautical applications, have been used to model the measured heat fluxes in energetic flame impingements. The applicability of those equations, to flame heating applications, has been determined. In aerospace applications, the vehicle moves through stagnant atmospheric gases. In impinging flames, the combustion products move around a stationary target. Therefore, the relative motion is similar in both applications. Besides hemi-nosed cylinders, flames impinging normal to cylinders [13] and plane surfaces [6, 10, 14] have been investigated. Such geometries are relevant to many industrial heating processes.

Chen and McGrath [15] reviewed impingement heat transfer from combustion products containing dissociated species. Sample heat transfer calculations were given for a stoichiometric O_2–C_3H_8 flame impinging on a 2 cm o.d. sphere. The equations recommended by McAdams [16], Rosner [17] and Altman and Wise [18] were used. The Lewis number, Le, is the ratio of the mass diffusion rate to the thermal diffusion effect. The results were evaluated for both $Le = 1$ and $Le > 1$. It was concluded that, for $Le = 1$, the existing information was sufficient to adequately predict heat transfer in chemically reacting systems. However, for flows in which $Le > 1$, more analytical and experimental work was recommended. Such systems are important for high temperature flames, where considerable dissociation occurs.

Two types of heat transfer behavior have been compared with experimental data, from the studies considered here (see Table 1). The first was forced convection, with no chemical dissociation. This is applicable in lower temperature-level flame impingements. The second was forced convection, with dissociation. The heat transfer relations for the second type have been variations of those recommended for the first type. These equations are useful in predicting the heat transfer in the absence of experimental data.

There are several objectives of this paper. The first is to present a comprehensive reference of semi-analytical heat transfer solutions, for impinging flames.

NOMENCLATURE

c_p	specific heat
d	diameter
h^C	chemical enthalpy
h^S	sensible enthalpy $= \int c_p \, dt$
h^T	total enthalpy $= h^C + h^S$
k	thermal conductivity
l	length
L	dimensionless distance between the burner and the stagnation body $= l_j/d_n$
Le	Lewis number
Pr	Prandtl number
q''	heat flux [kW m^{-2}]
r	radial distance from the burner centerline
Re	Reynolds number
t	temperature
Tu	turbulence intensity $= \sqrt{v'^2}/\bar{v}$
v	velocity
v'	fluctuating velocity.

Greek symbols

β	velocity gradient [s^{-1}]
Φ	surface catalytic efficiency
γ	turbulence-enhancement factor
μ	absolute or dynamic viscosity
Ω	oxygen enrichment ratio = oxygen volume in the oxidizer/total oxidizer volume
ϕ	equivalence ratio = stoichiometric oxygen/fuel volume ratio/actual oxygen/fuel volume ratio
ρ	density.

Subscripts

b	body or target
e	edge of boundary layer
i	species
∞	ambient
j	jet
n	nozzle
rec	evaluated at the recovery temperature
ref	evaluated at the reference temperature
s	stagnation point
w	wall.

This information will be useful to the designer, who needs to estimate the heat flux in a flame heating application. It will also be useful to the researcher. Future experimental results and semi-analytic solutions may be compared against the equations presented here. Another objective is to show how sample calculations, using the various solutions, compare to each other and to experimental data. The last objective is to show where information is lacking in the literature, and to suggest future areas for research.

2. HEAT TRANSFER MECHANISMS

Four general types of heat transfer mechanisms have been identified in the flame impingement studies reviewed here. They include convection, thermochemical heat release (TCHR), radiation and water vapor condensation. Semi-analytic solutions have been given only for forced convection, with and without TCHR. These mechanisms are discussed here. Natural convection, radiation, and water vapor condensation were considered, but were not found to be important. These mechanisms are discussed elsewhere [19].

2.1. *Forced convection flows*

In many conventional enclosed furnace heating processes, surface convection accounts for only a small fraction of the total heat transfer to the product. The vast majority of the heating comes from the radiation from the hot refractory walls. However, in flame impingement, with no furnace enclosure, forced convection may be 70–90% of the total heat flux [20, 21]. For flame temperatures up to about 1700 K, it is the dominant mechanism in impinging jet heat transfer [22]. In the studies reviewed here, laminar flames have been used most often [3–8, 10–12]. Turbulent flames have also been used [10, 12–14].

For low temperature flames, as common in air–fuel combustion systems, forced convection has generally been the only mechanism considered. This mechanism is sometimes referred to as *frozen* flow. That is, no

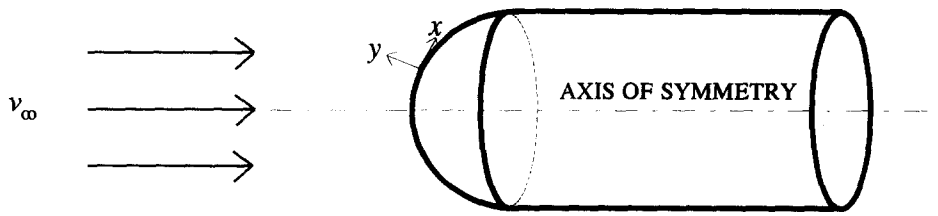

Fig. 1. Stagnation flow around a hemi-nosed, axisymmetric, body of revolution.

Table 1. Experimental studies using semi-analytical solutions

Target	Oxidizer	Re_n	ϕ	Fuel	β_s	d_b [mm]	v [m s^{-1}]	t_j [K]	Reference
Cylinder	Air	12 600	1.05	Natural gas	$2v_e/r_{0.5t}$	32.6–59.8	Not measured	Not measured	Hemeson *et al.* [13]
Flat plate	Air	1700–4250	1.0	Natural gas	v_e/d_b	Not given	Up to 50	Up to 2130	van der Meer [14]
	Air	7050–16 200	1.05	Natural gas	$v_e/r_{0.5t}$	5.6 dia.	Not measured	1643–2165	Horsley *et al.* [10]
	O_2	489–549	0.95–1.31	CH_4	v_e/d_j	152 × 152	40–49	2755–2925	Kilham and Purvis [8]
		551–692	1.45–1.83	C_3H_8					
Hemi-nosed cylinder	Air	Laminar[c]	0.5–0.63	H_2	$3v_e/d_b$	14	Not measured	1360–1450	Cookson and Kilham [3]
	Air	Laminar[c]	0.7–1.3	CO	$3v_e/d_b$	22.2	Not measured	1624–1910	Kilham and Dunham [4]
	Air	50–500	1.0	Natural gas	$3v_e/d_b$	12.7	Not given	2200	Conolly and Davies [6]
	O_2			CH_4, C_2H_4, C_3H_8, CO, H_2			9–17	2543–3144	
	Air	1200–10 000	1.0	CH_4	$(2.67+0.0926Tu)v_e/d_b$	22	2–3	1900–2100	Hargrave and Kilham [12]
	Air	12 600	1.05	Natural gas	$3v_e/r_{0.5t}$	50–150	Not measured	Not measured	Hemeson *et al.* [13]
	Air–O_2	Laminar[c]	0.62–1.14	CH_4	$3v_e/d_b$	9.5	Not given	2600–2763	Nawaz [7]
	O_2		0.83–1.70					2795–2996	
	Air–O_2	Laminar[a]	0.84–1.14	CH_4	$3v_e/d_b$	9.5	32–36	2710–2760	Fairweather *et al.* [11]
	O_2		0.83–1.70				35–38	2930–2990	
	O_2	Laminar[a]	0.95–1.31	CH_4	$3v_e/d_b$	9.5	21–32	2755–2925	Kilham and Purvis [5]
			1.45–1.83	C_3H_8					
	Air–O_2	Not given	0.95	Natural gas	$2.5v_e/d_b$	46	5–51	1640–2750	Ivernel and Vernotte [9]
	O_2						11–66	2300–2800	

[a] According to the author.
[c] Calculated from data in the reference.

heat release occurs from flame chemical reactions, at or near the target surface [5]. Even in highly dissociated oxygen–fuel flames, forced convection is still thought to be an important contributor to the overall heat transfer mechanisms. However, in the heat transfer solutions, forced convection has been combined with the TCHR.

2.2. *Thermochemical heat release* (TCHR)

This mechanism refers to the energy release which occurs when hot and dissociated gaseous species cool down, and exothermically recombine into more thermodynamically stable molecules. This mechanism has been given many names. It has commonly been referred to as *chemical* or *radical recombination*, or simply *recombination* [3–5, 8, 10, 11, 23–26]. Some referred to it as "convection vivre" or live convection [9, 13, 20, 21]. The term *aerothermochemistry* has been used in the aerospace field to describe the overall process [17]. That term incorporates the physical effects of the chemical reactions, with the fluid dynamics, in stagnation flows. This mechanism has also been referred to as the *exothermic displacement of equilibrium* [27]. The cooler solid body modifies the chemical equilibrium processes. Here, this mechanism will be referred to as *thermochemical* [17, 24] *heat release* or TCHR.

Many previous studies have identified the importance of this mechanism [3–5, 7, 8, 11, 24, 25]. The products of many combustion processes contain dissociated species. The level of such dissociation increases with the flame temperature. When a flame impinges on a cool surface, these species diffuse in the direction of the concentration gradients, toward the lower temperature regions. As the gases cool, they exothermically recombine with other such species, to form more stable molecules. These new components are thermodynamically favored, at lower temperature levels. For instance, when CH_4 is combusted adiabatically with pure O_2, significant amounts of unburned fuel in the form of CO (16 vol%) and H_2 (7 vol%) are produced, along with radicals like O (4 vol%), H (5 vol%) and OH (9 vol%). This composition was calculated, using a model developed for NASA [28]. As these combustion products cool to temperatures below about 1600 K, they react to form CO_2 and H_2O, while simultaneously releasing energy. However, when CH_4 is combusted with air, the final combustion products are essentially all CO_2, H_2O and N_2. The large concentration of N_2 acts as a heat sink, which lowers the flame temperature.

The heat release, from radical recombination, becomes important when high temperature dissociated gases contact cooler bodies. One example is the catalytic reaction of hydrogen atoms, to form stable H_2 molecules:

$$2H = H_2 + 431 \text{ Joules.} \quad (1)$$

H atom recombination was estimated to increase the heating rate by 30–90%, in fuel rich O_2–C_2H_2 flames [26]. In high temperature flame impingement, the combustion products diffuse through the boundary layer to the colder surface. They exothermically react and form new species. Two chemical mechanisms were found that initiate thermochemical heat release: equilibrium and catalytic. Nawaz referred to the combination, of those mechanisms, as mixed flow [7]. This is a mixture of equilibrium and catalytic chemistries.

2.2.1. *Equilibrium TCHR.* This has also been referred to as a *homogeneous* effect. The gas-phase chemical reactions occur in the boundary layer. Unstable species collide in the gas phase, with other atoms and molecules, which act as the third bodies in the chemical reactions. They initiate the reactions. The reaction time is much less than the time required for the gases to diffuse to the surface. Free radicals enter the laminar boundary layer by molecular diffusion [29]. The diffusion rate is small, compared to the chemical reaction rate. Therefore, the probability of homogeneous free-radical chemical reaction is high. In air–CH_4 flames, these reaction effects are negligible. However, combusting hydrocarbons with pure O_2 drastically increases the dissociation of the products. This is due to the high flame temperatures. Therefore, TCHR is more significant when O_2, instead of air, is used as the oxidizer. Kilham and Purvis [8] used heat flux gages to measure the heat flux in O_2–fuel flame impingement. The gages were made of silicon carbide (nearly non-catalytic) and platinum (highly catalytic), to try to measure the catalytic TCHR effects. No difference in heating rates was found. It was concluded that the TCHR occurred in the boundary layer, before reaching the surface. Therefore, it was assumed to be an equilibrium process.

2.2.2. *Catalytic TCHR.* This mechanism has also been called a *heterogeneous* effect. It involves chemical diffusion reactions at a surface. Radical species react, upon contact with the surface materials. The required chemical reaction time is much greater than the transit time, for the diffusing species to reach the surface. There is insufficient time for the radical species to react, before reaching the surface. Depending on the diffusing species involved, some surface materials may catalytically accelerate this reaction. For turbulent boundary layers, there is a high probability of radicals reaching the surface, without reacting in the boundary layer [29]. These radicals then catalytically combine at the surface. This reaction is accelerated by the turbulence. This type of TCHR has sometimes been referred to as *frozen* [6, 8, 17]. Nonreacting flow, that is no TCHR, has also been referred to as frozen. The latter usage is recommended.

2.2.3. *Mixed TCHR.* This is a combination of equilibrium and catalytic TCHR. Some of the dissociated species in the flame may react within the boundary layer, before reaching the surface. Some of the species may react catalytically upon contact with the cool surface. Some dissociated species may also remain unreacted, after traveling through the boundary layer,

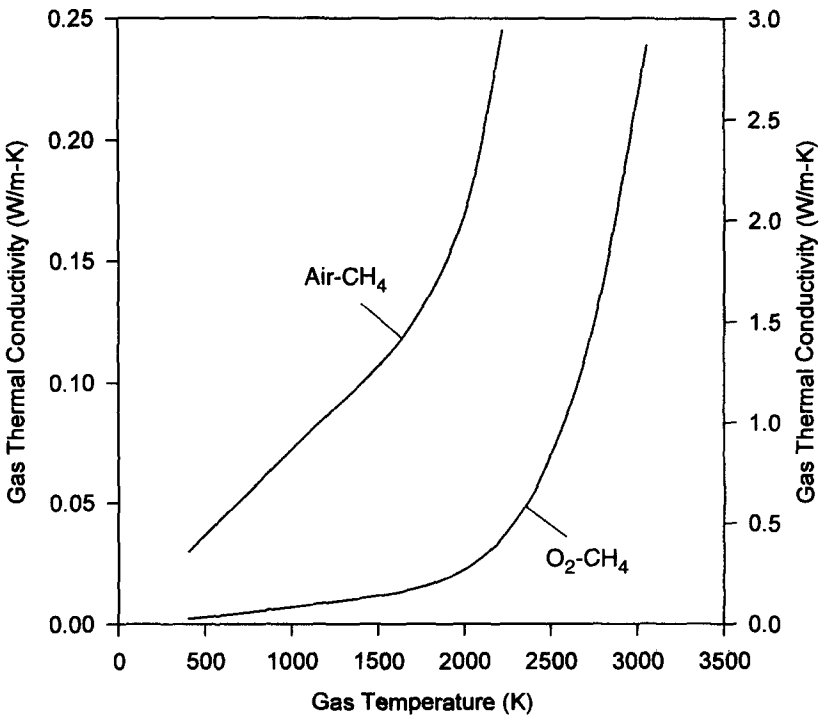

Fig. 2. The thermal conductivity of the combustion products from stoichiometric air–CH_4 (left-hand scale) and O_2–CH_4 (right-hand scale) flames, calculated using Gordon *et al.* [28, 34].

and after contacting the surface. This may occur if either the surface is not perfectly catalytic, or if not all of the gases reach the surface.

3. EQUATION PARAMETERS

The thermophysical properties and the stagnation velocity gradient have been used in all of the semi-analytic solutions. Many methods have been used to calculate these parameters. Those methods are discussed here, prior to presenting the semi-analytic solutions.

3.1. *Thermophysical properties*

These include the viscosity, density, thermal conductivity, Lewis number and the enthalpy of the gaseous combustion products. They are all temperature dependent. An example of this dependence, for the thermal conductivity, is shown in Fig. 2. The temperature of the combustion products varies with the oxygen enrichment ratio, Ω. For stoichiometric C_3H_8 flames, Chen [30] showed how the properties vary, as a function of Ω. Various methods have been used to evaluate the thermophysical properties. These methods are discussed below. The nomenclature is shown in Fig. 3.

In every semi-analytic solution, the gas temperature at the edge of the stagnation zone, t_e, has been used to evaluate some of the properties:

$$p_e = p(t_e) \tag{2}$$

where p is the property being evaluated. The wall temperature, at the stagnation point of the target, t_w, has also been used in every solution:

$$p_w = p(t_w). \tag{3}$$

Many studies [6, 8, 11–13] have used a weighted average, over the temperature range between the edge and the wall temperature, as

$$\bar{p} = \frac{\int_{t_w}^{t_e} p\,\mathrm{d}t}{t_e - t_w}. \tag{4}$$

The film, that is the mean temperature, between the edge and the wall temperatures, has commonly been used [4, 5, 9, 10]:

$$\bar{p} = p\left(\frac{t_e - t_w}{2}\right). \tag{5}$$

The reference temperature [31], has been used in several solutions [14, 32, 33]:

$$p_{ref} = p\{t_e + 0.5(t_w - t_e) + 0.22(t_{rec} - t_e)\} \tag{6}$$

where

$$t_{rec} = t_e + \frac{v_e^2 Pr_e^{0.5}}{2c_{p_e}}. \tag{7}$$

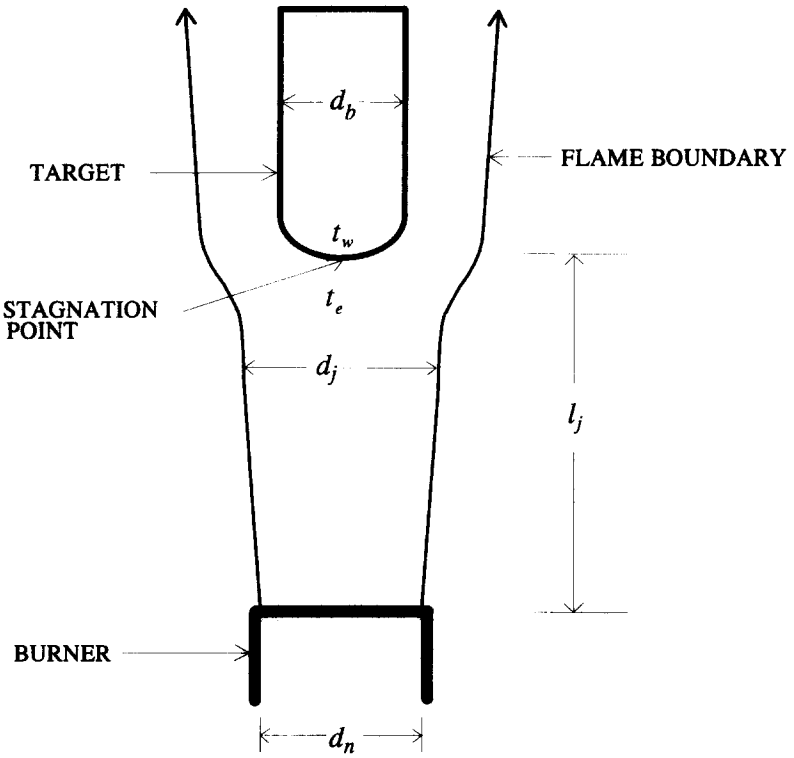

Fig. 3. Flame impingement on a hemi-nosed cylinder.

For low speed flows, $t_{rec} \approx t_e$, so $p_{ref} \approx \bar{p}$. Table 2 shows sample calculations, using the various methods, for the thermal conductivity of the combustion products.

3.2. *Stagnation velocity gradient*

The original semi-analytic heat transfer solution was developed for uniform external flows, impinging normal to a body of revolution [35]. The momentum equation for steady flow, in the boundary layer, along the surface of an axisymmetric body, and near the forward stagnation point [36], is:

$$v_x \frac{\partial v_x}{\partial x} + v_y \frac{\partial v_x}{\partial y} = \beta^2 x + v \frac{\partial^2 v_x}{\partial y^2}. \tag{8}$$

As shown in Fig. 1, x is the distance from the stagnation point, along the body, and y is the distance normal from the surface. From potential flow theory, near the forward stagnation point, the flow just outside the boundary layer may be given by [36]:

$$v_x = \beta x. \tag{9}$$

The constant β appears in the semi-analytic solutions for the heat flux at the forward stagnation point. At the edge of the stagnation zone, it is defined as:

$$\beta_s = \left(\frac{\partial v_x}{\partial x}\right)_{x=0, y=\delta} \tag{10}$$

where δ is the local boundary layer thickness at the axis of symmetry. This constant has been described in a variety of ways:

Table 2. Thermal conductivities for the equilibrium combustion products for stoichiometric CH_4 flames, calculated using Gordon *et al.* [28, 34]

Parameter	Units	Oxidizer Air	Oxidizer O_2
t_{AFT}	K	2220	3054
t_w	K	400	400
t_e	K	2000	2800
$\bar{t}$	K	1200	1600
t_{rec}	K	2000.6	2800.1
t_{ref}	K	1200.1	1600.0
k_w	W m^{-1} K^{-1}	0.0297	0.1546
k_e	W m^{-1} K^{-1}	0.1693	1.6818
$\bar{k}$	W m^{-1} K^{-1}	0.0860	0.1546
$\bar{k}$	W m^{-1} K^{-1}	0.0884	0.3288
k_{ref}	W m^{-1} K^{-1}	0.0860	0.1546

v_e assumed to be 50 m s^{-1}.

(1) velocity gradient at or near the stagnation point [7, 10, 25, 29, 37];
(2) stagnation velocity gradient [8, 11, 12, 24];
(3) velocity gradient in the radial direction, outside of the boundary layer, in the vicinity of the stagnation point [14, 32, 33];
(4) stagnation point radial velocity gradient [6, 13] and
(5) velocity gradient tangential to the potential flow [9].

This gradient has been determined analytically. It has

also been determined experimentally, as shown in Table 1.

3.2.1. *Analytical solutions.* The surface velocity gradient has been calculated for impinging flows normal to several stagnation body shapes. The solutions were developed using potential flow theory. This applies for high altitude flight, where the flow is approximately inviscid. The following relations have been computed [38, 39]:

$$\beta_s = 4v_e/d_b \quad \text{for a cylinder in crossflow} \quad (11)$$

$$= 3v_e/d_b \quad \text{for a sphere} \quad (12)$$

$$= 4v_e/\pi d_b \quad \text{for a disk.} \quad (13)$$

Most of the flame impingement studies, wherein the target was a hemi-nosed cylinder, assumed the value of β_s for a sphere. No analytical solution was available for the hemi-nosed cylinder. For an axisymmetric jet, impinging normal to an infinite plane, β_s has been analytically determined [37] as,

$$\beta_s = \frac{3\pi}{16}\frac{v_e}{d_j} \quad (14)$$

where d_j is the diameter of the jet at the edge of the stagnation zone (see Fig. 3). As shown in Fig. 1, the external velocity far from the body of revolution, v_∞, is uniform. In equations (11)–(14), the velocity at the edge of the boundary layer, v_e, is equal to v_∞. For flame impingement, the external flow is generally not uniform. This is especially true if the target is large, compared to the flame width. Therefore, v_e is commonly a function of the axial distance between the burner and the target, L. Then, for impinging flames, $v_e = v_e(x = 0, y = \delta)$.

3.2.2. *Empirical correlations.* In one study [10], β_s was experimentally determined as a function of $r_{0.5t}$. This is the radius at which the measured gas temperature is halfway between the maximum and the ambient, at a given axial location (see Fig. 4):

$$\frac{t_{r_{0.5t}} - t_\infty}{t_{max} - t_\infty} = 0.5. \quad (15)$$

In a related study [13], β_s was determined for flames impinging normal to a cylinder, a hemi-nosed cylinder, and a flat plate, using the same type of formulation. The results are shown in Table 3. Two forms of β_s were used. For the hemi-nosed cylinder, the calculated heat transfer, using β_{s1}, underpredicted the experimental measurements by up to 64%. The calculated heat transfer, using β_{s2}, only underpredicted the data by, at most, 29%. It overpredicted the data, by up to 54%. Hargrave and Kilham [12] determined β_s as a function of turbulence intensity, Tu. For laminar flow ($Tu = 0$), $\beta_s = 2.67\ v_e/d_b$. This is slightly lower than the value of β_s used in most of the hemi-nosed cylinder studies. In later studies, Hargrave and co-workers measured β_s for heated air impinging normal to a cylinder [40], and parallel to a hemi-nosed cylinder [41]. For the cylinder, β_s was empirically-determined as $\beta_s = 3.85 + 4.90Tu$. For the hemi-nosed cylinder, β_s was empirically-determined as $\beta_s = 2.67 + 9.62Tu$. These relations were then used in subsequent flame impingement studies [42, 43]. In those studies, empirical, not semi-analytic, heat transfer equations were determined. Therefore, those equations have not been included here. Van der Meer showed that $\beta_s = v_e/d_b$, for disks, applies within a distance of about five nozzle diameters from the burner outlet [14].

4. SEMI-ANALYTIC SOLUTIONS

This section discusses the early semi-analytic solutions for the heat transfer in stagnation flows. Sibulkin [35], Fay and Riddell [24] and Rosner [17] developed equations to compute the heat flux at the stagnation point of an axisymmetric body in a uniform, external, steady flow. Radiation effects were ignored. Sibulkin's equation included only the forced convection effect. Fay and Riddell and Rosner developed solutions, for both equilibrium and catalytic TCHR.

4.1. *Sibulkin*

The heat transfer at the forward stagnation point of a body of revolution was considered. The flow was uniform, except in the boundary layer. The flow around the body, in the boundary layer, was assumed to be laminar, incompressible, axisymmetric, and of low speed. Using the axisymmetric boundary layer equations, the following relation, for the local surface heat transfer was given [35]:

$$q_s'' = 0.763(\beta_s \rho_e \mu_e)^{0.5} Pr_e^{-0.6} c_{p_e}(t_e - t_w). \quad (16)$$

This applies for $0.6 < Pr_e < 2.0$. This formulation was actually developed for the hypersonic velocities common to space vehicle re-entry. It was assumed that the velocity is very low behind the bow shock wave, near the stagnation point, due to boundary layer flow conditions. The constant 0.763 was determined numeri-

Table 3. Stagnation velocity gradients used by Hemeson *et al.* [13]

Target	β_{s_1}	Predicted q_s''/ measured q_s''	β_{s_2}	Predicted q_s''/ measured q_s''
Cylinder	$2v_e/d_b$	—	$2v_e/r_{0.5t}$	0.59–1.18
Hemi-nosed cylinder	$3v_e/d_b$	0.36–1.0	$3v_e/r_{0.5t}$	0.71–1.54
Flat plate	—	—	$1.5v_e/r_{0.5t}$	0.56–0.91

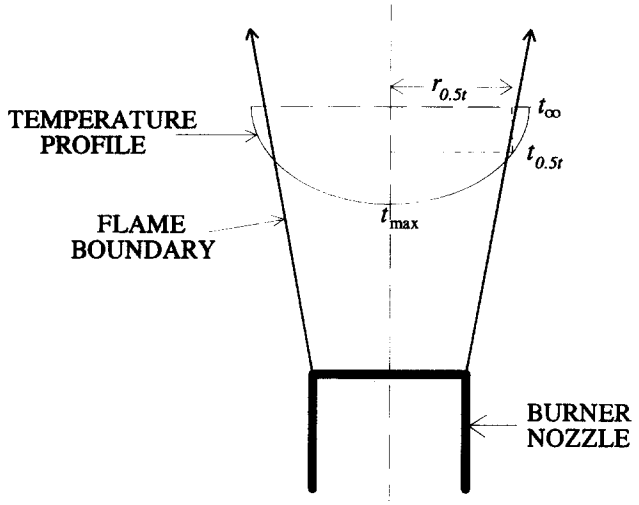

Fig. 4. Gas temperature profiles in a flame jet.

cally. All other semi-analytic solutions, presented here, are based on equation (16).

4.2. *Fay and Riddell*

They used the same axisymmetric boundary layer equations as Sibulkin. However, chemical dissociation was included. The driving force for heat transfer was enthalpy, instead of temperature. A factor was added, which contains the ratio of $\rho\mu$, evaluated at the wall and at the edge of the boundary layer. The heat transfer at the stagnation point was given as [24],

$$q_s'' = 0.76(\beta_s \rho_e \mu_e)^{0.5} \left(\frac{\rho_w \mu_w}{\rho_e \mu_e}\right)^{0.1} \times Pr_e^{-0.6} \left[1 + (Le_e^b - 1)\frac{h_e^C - h_w^C}{h_e^T}\right](h_e^T - h_w^T)$$

where

$$b = 0.52 \quad \text{for equilibrium TCHR} \tag{17}$$

$$= 0.63 \quad \text{for catalytic TCHR.} \tag{18}$$

Here, the exponent b varies, depending on the type of TCHR.

4.3. *Rosner*

In this formulation, the boundary layer equations were not solved directly, as had been done by Sibulkin and by Fay and Riddell. Instead, equation (16) was modified to include the effects of chemical dissociation. The resulting equation was then the sum of a forced convection term, from Sibulkin, and a diffusion–chemical reaction term. Two different forms of the solution were given, depending on the nature of the thermochemical heat release [17]. For equilibrium TCHR, the following form was recommended:

$$q_s'' = 0.763(\beta_s \rho_e \mu_e)^{0.5} \times Pr_e^{-0.6} \left[1 + (Le_e - 1)\frac{h_e^C - h_w^C}{h_e^T - h_w^T}\right]^{0.6} (h_e^T - h_w^T) \tag{19}$$

For catalytic TCHR, the recommended form was,

$$q_s'' = 0.763(\beta_s \rho_e \mu_e)^{0.5} \times Pr_e^{-0.6} \left[1 + (Le_e^{0.6} - 1)\frac{h_e^C - h_w^C}{h_e^T - h_w^T}\right](h_e^T - h_w^T). \tag{20}$$

For equilibrium TCHR, equation (19) differs significantly from that recommended by Fay and Riddell in equation (17). For catalytic TCHR, equation (20) is similar to that recommended in equation (18). It has commonly been assumed that the driving force for energy transport is the total enthalpy difference across the boundary layer. Rosner noted that this is a common misconception. It applies only for $Le_e = 1$, since the terms, inside the square brackets above, also contain the total and chemical enthalpy differences across the boundary layer. For $Le_e = 1$, equations (19) and (20) yield the same result. For the O_2–H_2 system, considered by Rosner, the calculated heat flux was very similar using either equation, across a realistic range of values. The application was rocket motors. For that system, it was not important whether the TCHR was equilibrium or catalytic. Rosner showed that the factor

$$\frac{h_e^C - h_w^C}{h_e^T - h_w^T}$$

becomes more important as the target temperature approaches the flame temperature ($t_w/t_e \to 1$). In that case, assuming $Le_e = 1$ may seriously underestimate the actual heat flux.

5. FLAME IMPINGEMENT EXPERIMENTS

This section discusses the impingement experiments (see Table 1) in which the measured heat flux was

compared to some form of a semi-analytic solution. There have been two types of experiments. The first was for lower temperature flames. There, forced convection is the dominant mechanism, TCHR is negligible. The second type was for higher temperature flames. There, forced convection and TCHR are both important. Both types are further classified into laminar and turbulent flow regimes.

5.1. *Forced convection (negligible TCHR)*

This mechanism has been important in air–fuel flames. In some studies [6, 12, 13], the driving potential was taken as $(h_e^T - h_w^T)$. For air–fuel flames, this is essentially the same as $(h_e^S - h_w^S)$.

5.1.1. *Laminar flow.* In one study [6], a wide range of heat fluxes was calculated (convection with and without TCHR) for several variations of equations (16)–(20). The best agreement, with the experimental data, was for:

$$q_s'' = 0.763(\beta_s \rho_e \mu_e)^{0.5} \frac{\bar{\bar{\mu}}}{\mu_e} \overline{\overline{Pr}}^{-0.6}(h_e^T - h_w^T). \quad (21)$$

The maximum deviation between this relation and the experimental data was 4%. Horsley *et al.* [10] recommended the following modification of equation (7):

$$q_s'' = 1.67(\beta_s \overline{\rho\mu})^{0.5} \overline{Pr}^{-0.6}(h_e^S - h_w^S) \quad (22)$$

This applies to $7050 \leqslant Re_n \leqslant 16\,200$. These values of Re_n are generally considered to be turbulent [2], even though the flames were described as having a "laminar appearance."

5.1.2. *Turbulent flow.* Horsley also inserted metal grids into industrial burners, to promote turbulence [10]. A similar modification of equation (16) was determined as,

$$q_s'' = 1.12(\beta_s \overline{\rho\mu})^{0.5} \overline{Pr}^{-0.6}(h_e^S - h_w^S). \quad (23)$$

This also applies to $7050 \leqslant Re_n \leqslant 16\,200$. The burner was located at the axial position, L, which yielded the maximum surface heat flux. The heat flux for the "laminar" flames, given in equation (22), is greater than the flux for the turbulent flames given in equation (23). Hargrave and Kilham [12] recommended the following relation:

$$q_s'' = 0.763(\beta_s \overline{\overline{\rho\mu}})^{0.5} \overline{\overline{Pr}}^{-0.6}(h_e^T - h_w^T). \quad (24)$$

It was shown that TCHR was not important. Therefore, all properties were evaluated at $Le = 1$. Equation (24) correlated the experimental data within 4%. Hemeson *et al.* [13] used a wide variety of burner designs. A range of cylinder and hemi-nosed cylinder diameters were tested. An equation, similar to (24), was suggested,

$$q_s'' = 0.763(\beta_s \overline{\overline{\rho\mu}})^{0.5} Pr_e^{-0.6}(h_e^T - h_w^T). \quad (25)$$

It was found that the heat flux did not depend on the radius of curvature, for the cylinder or for the hemi-nosed cylinder. The flux was dependent on the burner design. Van der Meer [14] used linear regression to correlate the experimental heat flux data as,

$$q_s'' = (1+\gamma)0.763(\beta_s \rho_{ref} \mu_{ref})^{0.5} Pr_{ref}^{-0.6}(h_e^S - h_w^S) \quad (26)$$

where γ = turbulence-enhancement factor. This was an experimentally determined function of $(Tu\ Re^{0.5})$. It varied from 0.0 for $Tu = 0$, up to about 0.4 for $Tu\ Re^{0.5} \simeq 30$.

5.2. *Forced convection with TCHR*

The combination of forced convection and TCHR has been most important in O_2–fuel flames. The total enthalpy difference has been used as the driving potential. Some of the equations also included the effect of Le. Figure 5 shows the importance of Le for O_2–CH_4 flames, especially at high temperatures.

5.2.1. *Laminar flow.* Cookson and Kilham [3] tested fuel–lean air–H_2 flames. Kilham and Dunham [4] tested fuel-lean to fuel-rich air–CO flames. A modified form of equation (20) was use in both studies. This included the catalytic TCHR effects, for multiple active species:

$$q_s'' = 0.763(\beta_s \rho_e \mu_e)^{0.5} \overline{Pr}^{-0.6} \times \left[1 + \sum_i^n \Phi_i (\overline{Le}_i^{0.6} - 1) \frac{h_{e,i}^C - h_{w,i}^C}{h_e^T - h_w^T}\right](h_e^T - h_w^T). \quad (27)$$

The surface catalytic efficiency, Φ_i, is a measure of the ability of the surface to act as a catalyst in a chemical reaction. A value of 0.0 means no radical species will catalytically react as a result of contacting the surface. A value of 1.0 means that all radical species will catalytically react, upon contacting the surface. In equation (27), a value of 1.0 was assumed. The actual value was not known. The quasi-equilibrium composition for air–H_2 mixtures was calculated, with a range of assumed concentrations of OH molecules [3]. The equilibrium components included H, H_2, H_2O, N_2, O, O_2 and OH. Using these concentrations, and the above equation, the heat flux as a function of OH concentration was calculated. By equating the calculated flux with the measured flux, the theoretical OH mole fraction was estimated to be 1.7% for $\phi = 0.5$ and 3% for $\phi = 0.63$. The experimental and calculated values were in excellent agreement, at the location in the flame where the atom concentrations (e.g., O) were negligible [44]. In general, the calculated values were shown to be highly dependent on the H, H_2, O and OH concentrations. Those concentrations were not measured. Using equation (27) and the measured total heat flux, the O concentration was estimated to be 2% by volume. Kilham and Purvis [5] measured the total heat flux from mostly fuel-rich flames. The data were compared to three different equations, using the recommendation by Fay and Riddell for $\rho_e \mu_e$. Only forced convection heat transfer was assumed in the first equation:

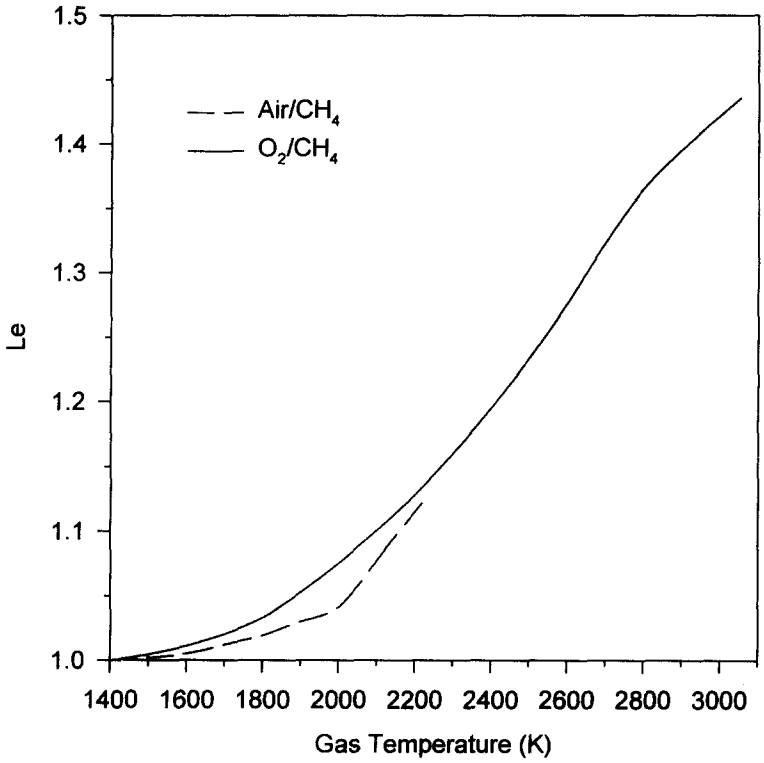

Fig. 5. Lewis number for the combustion products from stoichiometric air–CH_4 and O_2–CH_4 flames, calculated using Gordon *et al.* [28, 34].

$$q_s'' = 0.763(\beta_s\rho_e\mu_e)^{0.5}\left(\frac{\rho_w\mu_w}{\rho_e\mu_e}\right)^{0.1}\overline{Pr}^{-0.6}(h_e^S - h_w^S). \quad (28)$$

Equilibrium TCHR, with no Le augmentation ($Le = 1$), was assumed in the second equation:

$$q_s'' = 0.763(\beta_s\rho_e\mu_e)^{0.5}\left(\frac{\rho_w\mu_w}{\rho_e\mu_e}\right)^{0.1}\overline{Pr}^{-0.6}(h_e^T - h_w^T). \quad (29)$$

Equilibrium TCHR, with Le augmentation ($Le > 1$), was assumed in the third equation:

$$q_s'' = 0.763(\beta_s\rho_e\mu_e)^{0.5}\left(\frac{\rho_w\mu_w}{\rho_e\mu_e}\right)^{0.1}\overline{Pr}^{-0.6} \times\left[1+(Le_{e,H}-1)\frac{h_{e,H}^C - h_{w,H}^C}{h_e^T - h_w^T}\right]^{0.6}(h_e^T - h_w^T). \quad (30)$$

Equation (30) is a form of equation (19). Kilham showed that equation (19) could be simplified by calculating Le_e and $(h_e^C - h_w^C)$, based only on H atom recombination. Equation (28) underpredicted the experimental data by 24–42%. Equation (29) underpredicted the data by 3–7%. Equation (30) overpredicted the data by 2–10%. Conolly and Davies [6] used several variations of equations (16)–(20). A wide range of heat fluxes (forced convection with and without TCHR) were calculated. Equation (21) gave the best agreement with the experimental data. Nawaz [7] tested air–O_2–CH_4 ($\Omega = 0.46$–0.61) and O_2–CH_4 flames. Variations of equations (28)–(30) were used. For nonreacting flow, the relation was given as,

$$q_s'' = 0.763(\beta_s\rho_e\mu_e)^{0.5}\left(\frac{\rho_w\mu_w}{\rho_e\mu_e}\right)^{0.24}Pr_e^{-0.6}(h_e^S - h_w^S). \quad (31)$$

For equilibrium TCHR, with $Le = 1$, the relation was given as,

$$q_s'' = 0.763(\beta_s\rho_e\mu_e)^{0.5}\left(\frac{\rho_w\mu_w}{\rho_e\mu_e}\right)^{0.24}Pr_e^{-0.6}(h_e^T - h_w^T). \quad (32)$$

For equilibrium TCHR, with $Le > 1$, the relation was given as,

$$q_s'' = 0.763(\beta_s\rho_e\mu_e)^{0.5}\left(\frac{\rho_w\mu_w}{\rho_e\mu_e}\right)^{0.24} \times Pr_e^{-0.6}\left[1+(Le_{e,H}-1)\frac{h_{e,H}^C - h_{w,H}^C}{h_e^T - h_w^T}\right]^{0.6}(h_e^T - h_w^T). \quad (33)$$

The Le_e was calculated as the weighted average, between the flame temperature and 1600 K. Based on the experimental data, the flame was divided into two regions. The region closest to the burner was assumed to have radicals in excess of that predicted by ther-

modynamic equilibrium calculations. This is referred to as superequilibrium. All three equations seriously underpredicted the measured data in that region. The far region, at about $L > 0.7$, appeared to be in chemical equilibrium. In that region, equation (31) underpredicted the data by 17 to 77%, (32) underpredicted by 0.6–5.5% and (33) overpredicted by 1.0–3.5%. It was concluded that the flow was mixed TCHR. As in their earlier study [5], Kilham and Purvis [8] used three different equations to simulate various flow conditions. However, the Fay and Riddell recommendation for $\rho_e\mu_e$ was not used. The properties were also evaluated differently. The following relation was given for nonreacting flows:

$$q_s'' = 0.763(\beta_s\overline{\overline{\rho\mu}})^{0.5} Pr_e^{-0.6}(h_e^S - h_w^S). \quad (34)$$

This underpredicted the experimental data by 17–33%. The relation given for equilibrium TCHR, where $Le_e = 1$ was,

$$q_s'' = 0.763(\beta_s\overline{\overline{\rho\mu}})^{0.5} Pr_e^{-0.6}(h_e^T - h_w^T). \quad (35)$$

For the CH_4 flames and $\phi > 1.12$, this underpredicted the data by at most 2%. For $0.95 \leqslant \phi \leqslant 1.12$, it overpredicted the data by as much as 40%. For the C_3H_8 flames and $1.45 \leqslant \phi \leqslant 1.83$, it underpredicted the data by 1–40%. The relation given for equilibrium TCHR, with $Le_e > 1$ was,

$$q_s'' = 0.763(\beta_s\overline{\overline{\rho\mu}})^{0.5} Pr_e^{-0.6} \times\left[1+(Le_{e,H}-1)\frac{h_{e,H}^C - h_{w,H}^C}{h_e^T - h_w^T}\right]^{0.6}(h_e^T - h_w^T). \quad (36)$$

This overpredicted the data for both types of flames by as much as 48%. Fairweather *et al.* [11] tested air–O_2–CH_4 ($\Omega = 0.46$–0.61) and O_2–CH_4 flames. A modification of equation (16) was used:

$$q_s'' = 0.763(\beta_s\overline{\overline{\rho\mu}})^{0.5}\overline{\overline{Pr}}^{-0.6}(h_e^T - h_w^T). \quad (37)$$

This was an upper limit, when $Le > 1$. Equation (35) was used as a lower limit, when $Le = 1$. For $L > 0.8$, equation (35) underpredicted the data by up to 4%. Equation (37) overpredicted the data by up to 3%. For $L < 0.8$, equations (35) and (36) underpredicted the data by up to 40%. The experimental data generally fell between these two limits, except near the reaction zone. There, all predictions severely underestimated the heat flux, compared to the measurements. It was determined that the inclusion of only H atom reactions was a good approximation to including all possible radical reactions.

5.2.2. *Turbulent flow.* Ivernel and Vernotte [9] tested air–O_2–natural gas ($\Omega = 0.25$–0.90) and O_2–natural gas flames. Even though the flow regime was not specified, it appears to have been turbulent, based on a comparison with other studies [2]. A simplified form of equation (16) was used:

$$q_s'' = 0.763(\beta_s\rho_w\mu_w)^{0.5}\frac{\overline{Pr}^{0.4}}{Pr_w}(h_e^T - h_w^T). \quad (38)$$

This differs from the other semi-analytic solutions, since most of the properties are evaluated at the wall temperature. Equation (38) overpredicted the experimental data by up to 68%.

6. SAMPLE CALCULATIONS

Sample calculations are given here to compare the predicted heat flux, using the semi-analytic equations, with experimental measurements. The hemi-nosed cylinder is chosen as the target geometry, since it was used in nine of the 12 studies. Also, CH_4 is chosen as the fuel, since it was used in 10 of the 12 studies, either directly as methane, or indirectly as natural gas. In all of these studies, the flame was at or near stoichiometric conditions. The first set of calculations is for a stoichiometric air–CH_4 flame. This simulates forced convection without TCHR. Both laminar and turbulent conditions are modeled. The second set of calculations is for a stoichiometric O_2–CH_4 flame. This has been chosen to simulate forced convection with TCHR. Only laminar flames have been considered. This is due to the lack of both correlations and measurements for turbulent flames with TCHR. Tables 4–6 show the comparison between the measured and the computed heat fluxes, for the flames that have been modeled. The first section in each table lists the values for the important parameters, such as d_b, that are used in the computations. The measured

Table 4. Heat flux for laminar flames without TCHR

Parameter	Units	Conolly and Davies [6]	Hargrave and Kilham [12]
β_s	s^{-1}	$3v_e/d_b$	$2.67v_e/d_b$
d_b	mm	12.7	22
v_e	$m\ s^{-1}$	11	2.5
t_w	K	400	393
t_e	K	2200	2000
q_s'', measured	$kW\ m^{-2}$	265	110–210
q_s'', equation (21)	$kW\ m^{-2}$	272	81
q_s'', equation (26), $\gamma = 0$	$kW\ m^{-2}$	590	163
q_s'', equation (16)	$kW\ m^{-2}$	642	157
q_s'', equation (22)	$kW\ m^{-2}$	1225	356

Table 5. Heat flux for turbulent flames without TCHR

Parameter	Units	Hargrave and Kilham [12]
β_s, $Tu = 0.2$	s^{-1}	$2.7v_e/d_b$
d_b	mm	22
v_e	$m\ s^{-1}$	2.5
t_w	K	393
t_e	K	2000
q''_s, measured	$kW\ m^{-2}$	150–410
q''_s, equation (24)	$kW\ m^{-2}$	139
q''_s, equation (25)	$kW\ m^{-2}$	146
q''_s, equation (26), $\gamma = 0.4$	$kW\ m^{-2}$	229
q''_s, equation (23)	$kW\ m^{-2}$	240

heat flux is given next. Finally, the predictions are given in order of increasing heat flux.

6.1. *Laminar flames without TCHR*

Table 4 shows the measured and calculated heat fluxes, for a laminar flame without TCHR. The measured heat flux by Hargrave and Kilham [12] was from one set of tests at $Re_n = 2000$. The rest of those tests were done under turbulent flow conditions. Those results are discussed in the next section. As expected, the correlation by Conolly and Davies, in equation (21), closely matches their own experimental data. The other three correlations significantly overpredict the data. The heat flux measurements, by Hargrave and Kilham, varied widely with L. The fluxes calculated using equations (16) and (26) are within the measured range. Equation (22) overpredicts the Conolly and Davies experimental data by 360%. It overpredicts the Hargrave and Kilham data by up to 220%. Heat flux measurements from laminar, air–fuel flames, to hemi-nosed cylinders with a variety of diameters, have ranged from 73 to 460 $kW\ m^{-2}$ [2]. The results using equations (16), (22) and (26), for the Conolly and Davies conditions, exceed that range.

6.2. *Turbulent flames without TCHR*

The results for this case are shown in Table 5. The heat flux, measured by Hargrave and Kilham, varied widely with turbulence intensity, Tu, and with axial position, L. The predicted heat flux values, using equations (23) and (26), are within the measured range. Hargrave and Kilham recommended the relation given in equation (24). It underpredicts their own experimental data by 7–66%. Heat flux measurements from turbulent, air–fuel flames, to hemi-nosed cylinders of various diameters, have ranged from 100 to 580 $kW\ m^{-2}$ [2]. The calculations in Table 5 are all within that range.

6.3. *Laminar flames with TCHR*

The results for this case are given in Table 6. There is a wide variation in the predicted flux. However, most of the predictions, that incorporate TCHR, closely approximate the measurements. As expected, the correlations given in equations (28), (31) and (34), for nonreacting flow, significantly underpredict the data. The lowest heat flux prediction is for equation (28). It underpredicts the measurements by 44–58%. This is because the sensible, not the total, enthalpy difference was used as the driving force. The highest predictions are for equation (36). It overpredicts the measurements by 24–67%. The results using equations (33), (35) and (36) exceeded the range for the Nawaz [7] and Fairweather [11] measurements.

The heat flux calculated using Fay and Riddell's relation for equilibrium TCHR, in equation (17), was lower than that for catalytic TCHR, in equation (18). However, the predicted heat flux using Rosner's relation for equilibrium TCHR, in equation (19), was higher than that for catalytic TCHR, in equation (20). Therefore, no trend in the predictions is apparent, when comparing catalytic and equilibrium TCHR. Heat flux measurements from laminar, O_2–fuel flames, to hemi-nosed cylinders of various diameters, have ranged from 410 to 3700 $kW\ m^{-2}$ [2].

7. CONCLUSIONS

Twelve flame impingement experimental studies have been considered here. In those studies, the measured heat flux has been compared against one or more semi-analytic solutions. Cylindrical, flat plate, and hemi-nosed cylindrical targets have been used in one, three, and nine studies, respectively. Note that Hemeson *et al.* [13] used both a cylindrical target and a hemi-nosed cylinder target. Laminar flames have been used more often than turbulent flames.

Catalytic TCHR has been considered in only two studies [3, 4], as given in equation (27). An uncertainty is the lack of information on the surface catalytic efficiency, Φ, for given target materials. None of the studies compared the experimental results to both equilibrium and catalytic TCHR solutions. No semi-analytic solutions have been suggested for mixed TCHR.

Sample calculations for laminar and turbulent flows without TCHR, and laminar flows with TCHR, generally showed good agreement with the experimental data. However, in one case, the prediction was nearly five times the data. Therefore, caution must be used in the absence of any experimental data.

There are many possible explanations for the discrepancies between the predictions and the data. It has been assumed that the experimental data are reliable. However, none of the studies gave an estimate of the uncertainty in the measurements. In most cases, a complete set of data has not been given for a specific heat flux measurement. Commonly, a range of values, or an average value, for a particular variable, has been given. For example, Hargrave and Kilham [12] reported gas temperatures ranging from 1900 to 2100 K. No specific relationship, between those temperatures and the reported heat fluxes, was given. In

Table 6. Heat flux for laminar flames with TCHR

Parameter	TCHR type	Units	Kilham and Purvis [5]	Nawaz [7] Fairweather *et al.* [11]
β_s		s^{-1}	$3v_e/d_b$	$3v_e/d_b$
d_b		mm	9.5	9.5
v_e		m s^{-1}	27	37
t_w		K	380	360
t_e		K	2800	2900
q''_s, measured		kW m^{-2}	2530	2700–3640
q''_s, equation (21)		kW m^{-2}	1163	1520
q''_s, equation (28)		kW m^{-2}	1240	1520
q''_s, equation (31)		kW m^{-2}	1630	2030
q''_s, equation (34)		kW m^{-2}	1910	2440
q''_s, equation (29)		kW m^{-2}	1950	2580
q''_s, equation (27)	Catalytic	kW m^{-2}	2020	2690
q''_s, equation (30)	Equil.	kW m^{-2}	2100	2800
q''_s, equation (37)		kW m^{-2}	2340	3180
q''_s, equation (20)	Catalytic	kW m^{-2}	2510	3400
q''_s, equation (19)	Equil.	kW m^{-2}	2510	3410
q''_s, equation (32)		kW m^{-2}	2550	3450
q''_s, equation (17)	Equil.	kW m^{-2}	2560	3490
q''_s, equation (18)	Catalytic	kW m^{-2}	2600	3540
q''_s, equation (33)	Equil.	kW m^{-2}	2740	3760
q''_s, equation (35)		kW m^{-2}	3000	4140
q''_s, equation (36)	Equil.	kW m^{-2}	3230	4510

the sample calculations section of our paper, an average value of 2000 K was used. Another possible source of error, in the calculations, is the choice of β_s. In most cases, equation (12) for a sphere has been used, in the absence of an equation for a hemi-nosed cylinder. Also, the gases have been assumed to be at equilibrium conditions. In many cases, this is a reasonable assumption. However, Cookson and Kilham [3] and Kilham and Dunham [4] showed that the gases, in the region closest to their burner, were not in equilibrium. This could dramatically affect the properties used in the calculations.

For high temperature flames, where dissociation is important, the TCHR effects must be included. Otherwise, the predictions will significantly underpredict the data. Fay and Riddell [24] and Rosner [17] have developed solutions for both equilibrium and catalytic TCHR. However, the sample calculations in Table 6 showed that the results are nearly the same for either type of TCHR. Further work should determine if that would be true, over a wider range of conditions.

Acknowledgements—The authors would like to thank Air Products and Chemicals, Inc. for their support of this research.

REFERENCES

1. C. E. Baukal and B. Gebhart, A review of flame impingement heat transfer studies—I. Experimental conditions, *Combust. Sci. Technol.* **104,** 339–357 (1995).
2. C. E. Baukal and B. Gebhart, A review of flame impingement heat transfer studies—II. Measurements, *Combust. Sci. Technol.* **104,** 359–385 (1995).
3. R. A. Cookson and J. K. Kilham, Energy transfer from hydrogen–air flames, *Proceedings of Ninth International Symposium on Combustion*, pp. 257–263. Academic Press, New York (1963).
4. J. K. Kilham and P. G. Dunham, Energy transfer from carbon monoxide flames, *Proceedings of Eleventh International Symposium on Combustion*, pp. 899–905. The Combustion Institute, Pittsburgh, PA (1967).
5. J. K. Kilham and M. R. I. Purvis, Heat transfer from hydrocarbon–oxygen flames, *Combust. Flame* **16,** 47–54 (1971).
6. R. Conolly and R. M. Davies, A study of convective heat transfer from flames, *Int. J. Heat Mass Transfer* **15,** 2155–2172 (1972).
7. S. Nawaz, Heat transfer from oxygen enriched methane flames, Ph.D. Thesis, The University of Leeds, Leeds, U.K. (1973).
8. J. K. Kilham and M. R. I. Purvis, Heat transfer from normally impinging flames, *Combust. Sci. Technol.* **18,** 81–90 (1978).
9. A. Ivernel and P. Vernotte, Etude expérimentale de l'amélioration des transferts convectis dans les fours par suroxygénation du comburant, *Rev. Gén. Therm., Fr.* (210/211), 375–391 (1979).
10. M. E. Horsley, M. R. I. Purvis and A. S. Tariq, Convective heat transfer from laminar and turbulent premixed flames, *Heat Transfer* 1982 (Edited by U. Grigull, E. Hahne, K. Stephan and J. Straub, Vol. 3, pp. 409–415. Hemisphere, Washington, D.C. (1982).
11. M. Fairweather, J. K. Kilham and S. Nawaz, Stagnation point heat transfer from laminar, high temperature methane flames, *Int. J. Heat Fluid Flows* **5**(1), 21–27 (1984).
12. G. K. Hargrave and J. K. Kilham, The effect of turbulence intensity on convective heat transfer from premixed methane–air flames, *Instn Chem. Engng Symp. Ser.* **2**(86), 1025–1034 (1984).
13. A. O. Hemeson, M. E. Horsley, M. R. I. Purvis and A. S. Tariq, Heat transfer from flames to convex surfaces, *Instn Chem. Engng Symp. Ser.* **2**(86), 969–978 (1984).
14. T. H. van der Meer, Stagnation point heat transfer from turbulent low Reynolds number jets and flame jets, *Exper. Ther. Fluid Sci.* **4,** 115–126 (1991).

15. D. C. C. Chen and I. A. McGrath, Convective heat transfer in chemically reacting systems, *J. Inst. Fuel* **42**(336), 12–18 (1969).
16. W. H. McAdams, *Heat Transmission* (3rd Edn), Chap. 10. McGraw-Hill, New York (1954).
17. D. E. Rosner, Convective heat transfer with chemical reaction, Aeron. Res. Lab. Rept. ARL 99, Part 1, AD269816 (1961).
18. D. Altman and H. Wise, Effect of chemical reactions in the boundary layer on convective heat transfer, *Jet Propulsion* **26**(4), 256–269 (1956).
19. C. E. Baukal, L. K. Farmer, B. Gebhart and I. Chan, Heat transfer mechanisms in flame impingement heating, *Proceedings of the 1995 International Gas Research Conference* (Edited by D. A. Dolenc), Vol. 2, pp. 2277–2287. Government Institutes, Rockville, MD (1996).
20. J. M. Beér and N. A. Chigier, Impinging jet flames, *Combust. Flame* **12**, 575–586 (1968).
21. A. Milson and N. A. Chigier, Studies of methane–air flames impinging on a cold plate, *Combust. Flame* **21**, 295–305 (1973).
22. E. G. Jackson and J. K. Kilham, Heat transfer from combustion products by forced convection, *Ind. Engng Chem.* **48**(11) 2077–2079 (1956).
23. W. A. Gray, J. K. Kilham and R. Müller, *Heat Transfer from Flames*, p. 46. Elek Science, London (1976).
24. J. A. Fay and F. R. Riddell, Theory of stagnation point heat transfer in dissociated air, *J. Aero. Sci.* **25**, 73–85 (1958).
25. R. Viskanta, Heat transfer to impinging isothermal gas and flame jets, *Exper. Therm. Fluid Sci.* **6**, 111–134 (1993).
26. W. H. Giedt, L. L. Cobb and E. J. Russ, Effect of hydrogen recombination on turbulent flow heat transfer, ASME Paper 60-WA-256, New York (1960).
27. R. A. Cookson, An investigation of heat transfer from flames, Ph.D. Thesis, The University of Leeds, Leeds, U.K. (1960).
28. S. Gordon and B. J. McBride, Computer program for calculation of complex chemical equilibrium compositions, rocket performance, incident and reflected shocks, and Chapman–Jouget detonations, NASA report SP-273, Washington, D.C. (1971).
29. E. Buhr, G. Haupt and H. Kremer, Heat transfer from impinging turbulent jet flames to plane surfaces. In *Combustion Institute European Symposium* 1973 (Edited by F. J. Weinberg), pp. 607–612. Academic Press, New York (1973).
30. D. C. C. Chen, Improvement in convective heat transfer from hydrocarbon flames by oxygen enrichment, *J. Inst. Fuel* **45**(380), 562–567 (1972).
31. E. R. G. Eckert, Engineering relations for heat transfer and friction in high-velocity laminar and turbulent boundary-layer flow over surfaces with constant pressure and temperature, *J. Heat Transfer* **78**, 1273–1283 (1956).
32. C. J. Hoogendoorn, C. O. Popiel and T. H. van der Meer, Turbulent heat transfer on a plane surface in impingement round premixed flame jets, *Proceedings of the Sixth International Heat Transfer Conference*, Toronto, Vol. 4, pp. 107–112 (1978).
33. C. O. Popiel, T. H. van der Meer and C. J. Hoogendoorn, Convective heat transfer on a plate in an impinging round hot gas jet of low Reynolds number, *Int. J. Heat Mass Transfer* **23**, 1055–1068 (1980).
34. S. Gordon, B. J. McBride and F. J. Zeleznik, Computer program for calculation of complex chemical equilibrium compositions and applications. Supplement I: Transport properties, NASA Technical Memorandum 86885, Washington, D.C. (1984).
35. M. Sibulkin, Heat transfer near the forward stagnation point of a body of revolution, *J. Aero. Sci.* **19**, 570–571 (1952).
36. S. Goldstein, *Modern Developments in Fluid Dynamics*, p. 142. Dover Publications, New York (1965).
37. P. S. Shadlesky, Stagnation point heat transfer for jet impingement to a plane surface, *AIAA J.* **21**(8), 1214–1215 (1983).
38. T. H. van der Meer, Heat transfer from impinging flame jets, Ph.D. Thesis, Technical University of Delft, the Netherlands (1987).
39. W. M. Kays and M. E. Crawford, *Convective Heat and Mass Transfer* (2nd Edn), p. 141. McGraw-Hill, New York (1980).
40. G. K. Hargrave, M. Fairweather and J. K. Kilham, Turbulence enhancement of stagnation point heat transfer on a circular cylinder, *Int. J. Heat Fluid Flow* **7**(2), 89–95 (1986).
41. G. K. Hargrave, M. Fairweather and J. K. Kilham, Turbulence enhancement of stagnation point heat transfer on the body of revolution, *Int. J. Heat Fluid Flow* **6**(2), 91–98 (1985).
42. G. K. Hargrave, M. Fairweather and J. K. Kilham, Forced convective heat transfer from premixed flames—I. Flame structure, *Int. J. Heat Fluid Flow* **8**(1), 55–63 (1985).
43. G. K. Hargrave, M. Fairweather and J. K. Kilham, Forced convective heat transfer from premixed flames—II. Impingement heat transfer, *Int. J. Heat Fluid Flow* **8**(2), 132–138 (1985).
44. P. G. Dunham, Convective heat transfer from carbon monoxide flames, Ph.D. Thesis, The University of Leeds, Leeds, U.K. (1963).